One-dimensional, weakly nonlinear electromagnetic solitary waves in a plasma

H. H. Kuehl
University of Southern California, Los Angeles, California 90089-0271

C. Y. Zhang
University of California at Los Angeles, Los Angeles, California 90024

(Received 10 March 1993)

The properties of one-dimensional, weakly nonlinear electromagnetic solitary waves in a plasma are investigated. The solution of the resulting eigenvalue problem shows that the solitary waves have amplitudes which are allowed discrete values only and their vector and scalar potentials are proportional to ω_p/ω_0 and $(\omega_p/\omega_0)^2$, respectively, where ω_p and ω_0 are the plasma and electromagnetic wave frequencies, respectively. Their widths are comparable to the plasma wavelength $\lambda_p = 2\pi c/\omega_p$ (where c is the velocity of light), except for the lowest-order solitary wave, whose width is large compared with λ_p, which is a true wakeless solitary wave only in the limit of vanishing amplitude. Simple analytical solutions are derived for higher-order solitary waves, whose vector-potential envelope is highly oscillatory, and are shown to consist, in the group-velocity frame, of two trapped, oppositely traveling waves.

PACS number(s): 52.35.Mw, 52.35.Sb, 52.40.Db, 52.40.Nk

I. INTRODUCTION

A high-power laser pulse propagating through a plasma produces a wide variety of interesting phenomena. These include plasma wake-field generation, relativistic self-focusing, frequency shifts, and harmonic generation [1–7]. Another important area of nonlinear laser-plasma phenomena, and more generally, nonlinear electromagnetic wave-plasma phenomena, which has received inadequate attention, is that of solitary waves. Gersten and Tzoar [8], Tsintsadze and Tskhakoya [9], and Yu, Shukla, and Spatschek [10] have investigated electromagnetic solitary waves in a plasma in the quasineutrality approximation i.e., the charge separation due to excitation of the longitudinal plasma wave by the ponderomotive force was neglected. Rao, Varma, Shukla, and Yu [11] included charge separation but considered only solitary waves whose speed is comparable to the ion-acoustic speed, i.e., both electron temperature and ion motion are important. We consider here, however, the regime in which the solitary wave speed is close to the velocity of light c, the electron temperature is negligible because the directed motion of the electrons is assumed to be much larger than the thermal motion, and the ion motion is negligible because the pulse length l is sufficiently short to satisfy $\omega_{pi} l/c \ll 1$, where ω_{pi} is the ion plasma frequency. Moreover, charge separation is not neglected. Indeed, the solitary wave solutions we obtain would not exist without the charge separation produced by the nonlinear coupling of the transverse electromagnetic wave to the longitudinal plasma wave. Electromagnetic solitary waves in the regime considered here have also been investigated by Koslov, Litvak, and Suvorov [12] and Kaw, Sen, and Katsouleas [13]. Both of these investigations consist primarily of the study of the properties of intense, strongly nonlinear electromagnetic pulses in which the particle oscillation velocities are comparable with the velocity of light. In the present work, however, the focus is on weakly nonlinear pulses wherein the electron motion is only weakly relativistic. In that case the coupled equations governing the pulse behavior are considerably simpler than in the strongly nonlinear case. Because of this, several general properties regarding pulse length, amplitude, and speed of weakly nonlinear solitary waves emerge naturally from the analysis which are not apparent from the more general equations valid for strongly nonlinear pulses. Moreover, although in general the governing equations must be solved numerically, a simple approximate analytical solution is derived for the case in which the vector potential envelope is highly oscillatory. Thus, the present work complements the strongly nonlinear results of Refs. [12] and [13].

II. ANALYSIS

To lowest order, the normalized vector and scalar potentials of a linearly polarized, weakly nonlinear laser pulse in a plasma are governed by the coupled equations [14]

$$2iA_{1\tau}^{(1)} + \Omega_p^2 A_{1\xi\xi}^{(1)} + \Omega_p^2 \phi_0^{(2)} A_1^{(1)} = 0 , \tag{1}$$

$$\phi_{0\xi\xi}^{(2)} + \Omega_p^2 \phi_0^{(2)} = \Omega_p^2 |A_1^{(1)}|^2 , \tag{2}$$

where $A_1^{(1)}$ is the first-order vector-potential envelope normalized (in SI units) to $m_0 c/e$, and $\phi_0^{(2)}$ is the second-order scalar potential normalized to $m_0 c^2/e$, where m_0, e, and c are the electron rest mass and charge and the velocity of light, respectively. The complete representation of the potentials are [14]

$$A = \sum_{m=1}^{\infty} \sum_{l=-\infty}^{\infty} \epsilon^m A_l^{(m)}(\xi,\tau) \exp(il\theta) , \tag{3}$$

$$\phi = \sum_{m=2}^{\infty} \sum_{l=-\infty}^{\infty} \epsilon^m \phi_l^{(m)}(\xi,\tau) \exp(il\theta) , \tag{4}$$

and

$$\xi=\epsilon(Z-\Omega_0'T)\ , \quad \tau=\epsilon^4 T, \quad \theta=Z-\Omega_0 T\ . \tag{5}$$

The normalized spatial coordinate and time are defined by $Z=k_0 z$ and $T=k_0 ct$, where z is the spatial coordinate, t is the time, and k_0 is the carrier wave number in the absence of any nonlinear interaction with the plasma. The normalized wave number, frequency, and plasma frequency are defined by $K=k/k_0$, $\Omega=\omega/k_0 c$, and $\Omega_p=\omega_p/k_0 c$. In terms of these variables, the linear dispersion relation is

$$\Omega^2=K^2+\Omega_p^2\ . \tag{6}$$

Because of this normalization, the normalized fundamental laser wave number is $K_0=1$, and in Eq. (5), the corresponding normalized frequency Ω_0 and group velocity Ω_0' based on the linear dispersion relation (6) are given by $\Omega_0=\Omega(K=1)=(1+\Omega_p^2)^{1/2}$ and $\Omega_0'=(\partial\Omega/\partial K)_{K=1}=\Omega_0^{-1}$. The expansions (3) and (4), and the resulting Eqs. (1) and (2) are based on the assumption that the lowest-order vector potential and the normalized plasma frequency Ω_p are of order ϵ, which is the formal expansion parameter.

The solution of Eqs. (1) and (2) is simplified if the variables are scaled according to

$$A_1=A_1^{(1)}/\Omega_p, \quad \Phi_2=\phi_0^{(2)}/\Omega_p^2\ , \tag{7}$$

$$\xi'=\Omega_p\xi, \quad \tau'=\Omega_p^4\tau\ , \tag{8}$$

whereby Eqs. (1) and (2) become

$$2iA_{1\tau'}+A_{1\xi'\xi'}+\Phi_2 A_1=0\ , \tag{9}$$

$$\Phi_{2\xi'\xi'}+\Phi_2=|A_1|^2\ , \tag{10}$$

which are *independent* of Ω_p. We look for solitary wave solutions of the form

$$A_1(\xi',\tau')=R_1(\xi')\exp(i\Lambda\tau'/2)\ , \tag{11}$$

where $R_1(\xi')$ is real and Λ is a real constant corresponding physically to a frequency shift. Equations (9) and (10) become

$$R_{1\xi'\xi'}+(\Phi_2-\Lambda)R_1=0\ , \tag{12}$$

$$\Phi_{2\xi'\xi'}+\Phi_2=R_1^2\ . \tag{13}$$

Within the framework of Eqs. (12) and (13) it may be verified that, as in the strongly nonlinear case treated in Ref. [12], two types of solitary waves are possible. Type I has symmetrical R_1 and Φ_2 as defined by $R_1(\xi')=R_1(-\xi')$, $\Phi_2(\xi')=\Phi_2(-\xi')$, whereas type II has antisymmetric R_1 and symmetric Φ_2 defined by $R_1(\xi')=-R_1(-\xi')$, $\Phi_2(\xi')=\Phi_2(-\xi')$. In order to find these solitary wave solutions, which must satisfy R_1, $\Phi_2\rightarrow 0$ as $|\xi'|\rightarrow\infty$, it is noted that, for sufficiently large positive ξ' where $\Phi_2\ll\Lambda$, the proper asymptotic solutions of Eqs. (12) and (13) are $R_1=C_1\exp(-\Lambda^{1/2}\xi')$ and $\Phi_2=C_1^2(4\Lambda+1)^{-1}\exp(-2\Lambda^{1/2}\xi')$, where C_1 is a constant. The numerical procedure is to start the solution at large positive ξ' with these exponential forms for R_1 and Φ_2 and then integrate the system (12) and (13) in the negative ξ' direction until some point ξ' is found where both $dR_1/d\xi'$ and $d\Phi_2/d\xi'$ vanish simultaneously (type-I solitary wave), or R_1 and $d\Phi_2/d\xi'$ vanish simultaneously (type-II solitary wave). It was found numerically that these conditions occur only for particular values of Λ, i.e., Λ is the eigenvalue and the corresponding R_1 and Φ_2 are the eigenfunctions. Figures 1 and 2 show the first nine eigenfunctions of both R_1 and Φ_2, where N denotes the number of half cycles of R_1. Table I shows the eigenvalues Λ for the first nine solitary waves. It is evident that the vector-potential eigenfunctions become increasingly oscillatory with increasing eigenvalue, whereas the scalar potential eigenfunctions are typically bell-shaped with a single maximum. Also, the amplitudes of both vector and scalar potentials increase with increasing eigenvalue. These properties are qualitatively similar to those of the strongly nonlinear regime [12,13]. It should be emphasized, however, that for the weakly nonlinear regime considered here, Figs. 1 and 2 represent universal curves for solitary wave profiles valid for arbitrary $\Omega_p=\omega_p/k_0 c\approx\omega_p/\omega_0\ll 1$. To obtain the actual normalized vector- and scalar potential profiles, it is only necessary to multiply the ordinates in Figs. 1 and 2 by Ω_p and Ω_p^2, respectively, because of the scaling given by Eq. (7). This simple scaling does not exist in the strongly nonlinear case.

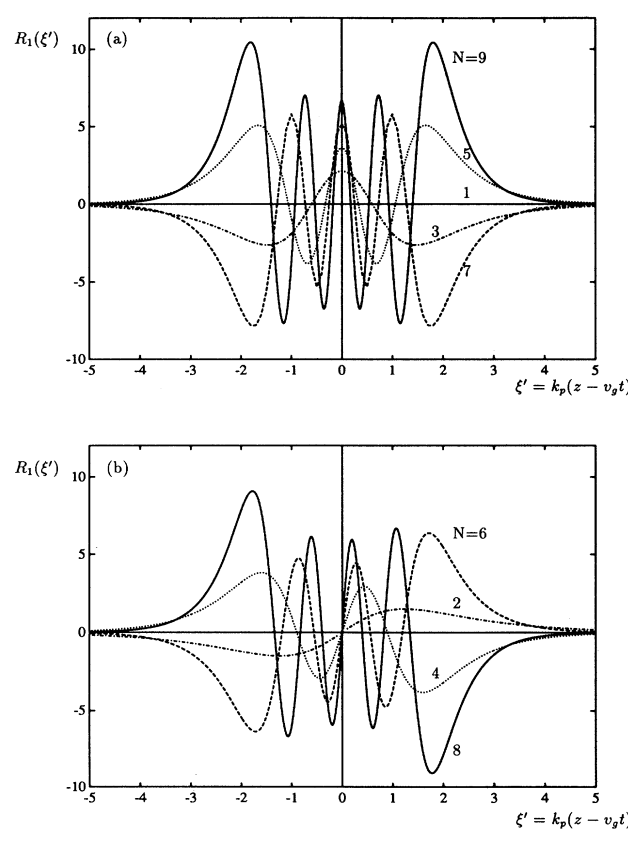

FIG. 1. Normalized vector-potential envelope $R_1(\xi')$ for (a) type-I solitary wave (even symmetry) and (b) type-II solitary wave (odd symmetry).

TABLE I. Eigenvalues Λ for the lowest nine electromagnetic solitary waves.

N	Λ
1	0.00
2	0.50
3	0.975
4	1.47
5	2.00
6	2.55
7	3.13
8	3.70
9	4.28

Several other interesting properties of these electromagnetic solitary waves in a plasma are apparent from Figs. 1 and 2. From the definition of ξ' given by Eq. (8), it follows that $\xi' = k_p(z - v_{gl}t)$, where the plasma wave number is $k_p = \omega_p / c = 2\pi/\lambda_p$, the linear group velocity is $v_{gl} = c/(1+\omega_p^2/k_0^2c^2)^{1/2}$, and z and t are the (unnormalized) spatial coordinate and time, respectively. It is evident from Figs. 1 and 2 that each solitary wave (except the $N=1$ case discussed subsequently) has a width given approximately by $\Delta\xi' = k_p \Delta z \approx 6$. Therefore, except for the $N=1$ case, every weakly nonlinear, one-dimensional, electromagnetic solitary wave in a plasma has a spatial width Δz which is comparable to the plasma wavelength λ_p, which clearly show the important role which the (nonlinear) coupling of the laser pulse to the longitudinal plasma wave plays in the existence of these solitary wave solutions. It may also be noted that the condition $\omega_{pi}\Delta z / c \ll 1$, necessary for the neglect of ion motion, is satisfied because $\Delta z \approx \lambda_p = 2\pi c/\omega_p$ and therefore $\omega_{pi}\Delta z / c \approx (m_e/m_i)^{1/2} \ll 1$. The $N=1$ solitary wave is the only solution whose width is large compared with the plasma wavelength. In this case, the quasineutrality condition $|\Phi_{2\xi'\xi'}| \ll \Phi_2$ applies, so that Eq. (10) gives $\Phi_2 \approx |A_1|^2$, whereby Eq. (9) becomes the nonlinear Schrödinger (NLS) equation,

$$2iA_{1\tau'} + A_{1\xi'\xi'} + |A_1|^2 A_1 = 0 , \tag{14}$$

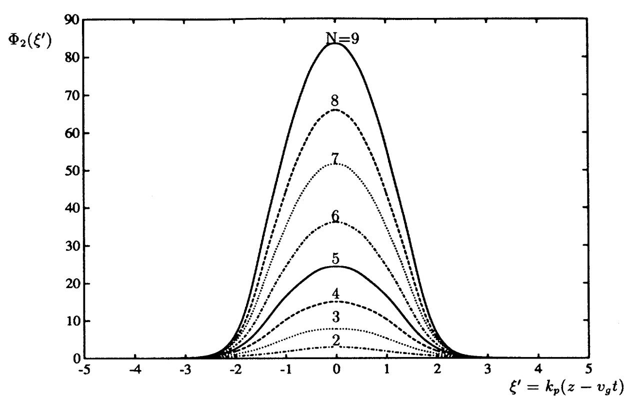

FIG. 2. Normalized scalar potential $\Phi_2(\xi')$ corresponding to the vector potential of Fig. 1.

whose simplest solitary wave solution is

$$A_1 = A_0 \operatorname{sech}(A_0\xi'/2^{1/2}) \exp(iA_0^2\tau'/4) , \tag{15}$$

where A_0 is an arbitrary constant. Comparison of Eq. (11) with Eq. (15) shows that for this case the eigenvalue is $\Lambda = A_0^2/2$. It is interesting to note, however, that for large negative ξ' the solution of Eq. (10) with A_1 given by Eq. (15) is $\Phi_2 = -4\pi \exp(-\pi/2^{1/2}A_0)\sin(\xi')$, which represents the wake of longitudinal plasma oscillations left behind the laser pulse. Because a solitary wave must, by definition, vanish for $|\xi'| \to \infty$, (i.e., it must be wakeless), it follows that, in a strict mathematical sense, Eq. (15) represents a true solitary wave only in the limit $\Lambda = A_0^2/2 \to 0$, i.e., it must have vanishing amplitude and infinite width. Because of this, Table I gives $\Lambda = 0$ and Fig. 1(a) shows $R_1 = 0$ for the $N=1$ case. Of course, from a less rigorous point of view, Eq. (15) does represent a long-pulse solitary wave (width $\gg \lambda_p$) whose wake can be made negligibly small if A_0 is sufficiently small.

A distinctive property of the solitary wave solutions of Eqs. (9) and (10) is that, for each eigenvalue Λ, both the shape and amplitude of the corresponding eigenfunction is completely determined. This property differs from that of several well-known nonlinear equations, such as the NLS equation or the Korteweg–de Vries equation which allow solitary wave solutions with a continuous range of amplitude. For example, the solitary wave solution (15) of the NLS equation (14) is valid for arbitrary values of the amplitude A_0, i.e., the shape is determined but the amplitude is arbitrary. Thus, the discrete amplitudes allowed by Eqs. (9) and (10) are in contrast to the continuous amplitude range of solitary waves allowed by several well-known nonlinear equations. This discrete amplitude property is also found in the strongly nonlinear case [12,13].

The previous analysis focuses on the lowest-order vector and scalar potentials. The next-higher-order contributions in the series (3) and (4) involve $A_1^{(2)}$ and $\phi_0^{(3)}$ which are governed by Eqs. (61) and (66) of Ref. [14], which, with the definitions $A_2 = A_1^{(2)}/\Omega_p^2 = R_2(\xi')\exp(i\Lambda\tau'/2)$ and $\Phi_3 = \phi_0^{(3)}/\Omega_p^3$, can be written as

$$R_{2\xi'\xi'} + (\Phi_2 - \Lambda)R_2 = -i\Lambda R_{1\xi'} - \Phi_3 R_1 , \tag{16}$$

$$\Phi_{3\xi'\xi'} + \Phi_3 = R_1(R_2 + R_2^*) . \tag{17}$$

Letting $R_2 = \alpha_2 + i\beta_2$, where α_2 and β_2 are real, Eqs. (16) and (17) yield

$$\alpha_{2\xi'\xi'} + (\Phi_2 - \Lambda)\alpha_2 = -\Phi_3 R_1 , \tag{18}$$

$$\beta_{2\xi'\xi'} + (\Phi_2 - \Lambda)\beta_2 = -\Lambda R_{1\xi'} , \tag{19}$$

$$\Phi_{3\xi'\xi'} + \Phi_3 = 2R_1\alpha_2 . \tag{20}$$

A solution of Eqs. (18) and (20) is $\alpha_2 = \Phi_3 = 0$. The solution of Eq. (19) can be shown to be $\beta_2 = -\Lambda\xi' R_1/2$, whereby we obtain

$$A_2 = -i(\Lambda/2)\xi' R_1 \exp(i\Lambda\tau'/2) . \tag{21}$$

Using $A_1^{(1)} = \Omega_p A_1$, $A_1^{(2)} = \Omega_p^2 A_2$ together with Eq. (3)

with $\epsilon=1$, and noting that $A_2^{(2)}=0$ [14], the normalized vector potential through second order is $A=(A_1^{(1)}+A_1^{(2)})\exp(i\theta)+\text{c.c.}$ which, using Eqs. (5), (8), (11), and (21), becomes

$$\begin{aligned} A &= \Omega_p R_1(\xi')(1-i\Lambda\Omega_p\xi'/2)\exp[i(\Lambda\tau'/2+\theta)]+\text{c.c.} \\ &\approx \Omega_p R_1(\xi')\exp\{i[\Lambda(\tau'-\Omega_p\xi')/2+\theta]\}+\text{c.c.} \\ &= \Omega_p R_1(\xi')\exp[i(KZ-\Omega T)]+\text{c.c.}, \end{aligned} \tag{22}$$

where we have used $1-i\Lambda\Omega_p\xi'/2\approx\exp(-i\Lambda\Omega_p\xi'/2)$, which is valid through second order in Ω_p. The normalized wave number K and frequency Ω are given by

$$K=1-\Lambda\Omega_p^2/2 , \tag{23}$$

$$\begin{aligned} \Omega &= \Omega_0[1-\Lambda\Omega_p^2(\Omega_0'+\Omega_p^2)/2\Omega_0] \\ &\approx 1+\Omega_p^2/2-\Lambda\Omega_p^2/2 , \end{aligned} \tag{24}$$

where Eq. (24) has been evaluated through second order in Ω_p using the expansions $\Omega_0=(1+\Omega_p^2)^{1/2}=1+\Omega_p^2/2+\cdots$ and $\Omega_0'=(1+\Omega_p^2)^{-1/2}=1-\Omega_p^2/2+\cdots$. It may be verified that Ω and K given by Eqs. (23) and (24) satisfy the linear dispersion relation (6) through second order in Ω_p. It is evident from Eqs. (23) and (24) that the wave number and frequency are shifted from their linear values by an amount proportional to $\Omega_p^2\Lambda$, which is a nonlinear effect because the solitary wave amplitude is proportional to Ω_p, according to Eq. (22). Moreover, the wave-number and frequency shifts are larger for solitary waves whose envelopes have more oscillations (larger N) because, as in evident from Table I, their eigenvalues Λ are larger. In spite of the frequency and wave-number shifts, Eqs. (23) and (24) yield a normalized phase velocity $v_p=\Omega/K=1+\Omega_p^2/2$, which is the linear value of the normalized phase velocity Ω_0 through second order. Because Eqs. (5), (8), and (22) show that the pulse envelope travels with the linear group velocity $v_g=\Omega_0'\approx 1-\Omega_p^2/2$, the normalized group and phase velocities satisfy

$$v_g v_p=1 , \tag{25}$$

which is valid through order Ω_p^2. The result that the phase and group velocities through order Ω_p^2 are unchanged from their linear values can be understood from the linear dispersion relation (6) which shows that a wave-number shift of order Ω_p^2, as in Eq. (23), produces a phase and group-velocity shift of order Ω_p^4. This implies that in order to investigate any modifications of the group or phase velocities from their linear values within the framework of the perturbation expansion used here, it would be necessary to carry it out through order Ω_p^4..

In the related investigation of Kozlov, Litvak, and Surorov [12] two basic restrictions are imposed at the outset. The first is that the solitary wave envelope is a function of a single variable $z-v_g t$. This appears to be in disagreement with the expansion assumed in Eq. (3), where $A_l^{(m)}(\xi,\tau)$ represents the mth-order contribution to the envelope of the lth harmonic. Since Eqs. (11) and (21) show that $A_1^{(1)}$ and $A_1^{(2)}$ are functions of both $\xi'\propto(z-v_g t)$ and $\tau'\propto t$, they do not satisfy the first condition in Ref. [12]. However, by absorbing the exponential part of the τ' and ξ' dependence of $A_1^{(1)}+A_1^{(2)}$ into the carrier $\exp(i\theta)$, one obtains a redefined carrier $\exp[i(KZ-\Omega T)]$ and envelope $\Omega_p R_1(\xi')$ as shown in Eq. (22), which does indeed satisfy the first condition of Ref. [12]. The second basic restriction of Ref. [12] is that $v_b v_p=c^2$, which, according to Eq. (25), is also satisfied by our solutions. Thus, it is interesting that, in the weakly nonlinear case treated here, it is not necessary to separately impose the two basic restrictions of Ref. [12] because they emerge as consequences of the analysis.

III. SOLITARY WAVES FOR $N\gg 1$

When $N\gg 1$, Figs. 1 and 2 show that R_1 varies rapidly compared with Φ_2. Under this condition, an approximate solution of Eq. (12) is the WKB solution given by [15]

$$R_1=C_N\Psi^{-1/4}\sin\left[\int_0^{\xi'}\Psi^{1/2}d\xi'-N\pi/2\right] , \tag{26}$$

where C_N is an arbitrary constant, and

$$\Psi=\Phi_2-\Lambda , \tag{27}$$

which must satisfy the condition

$$\int_{-\xi_0'}^{\xi_0'}\Psi^{1/2}d\xi'=(2N-1)\pi/2,\quad N=1,2,3,\ldots, \tag{28}$$

where Ψ vanishes at the turning points $\pm\xi_0'$ defined by

$$\Psi(\pm\xi_0')=0 . \tag{29}$$

Equation (26) is valid inside and not too near the turning points. Since Ψ is still to be determined, the locations of the turning points are unknown at this point. In order to obtain ξ_0', C_N, and Ψ self-consistently, Eq. (26) is inserted into Eq. (13) with the result

$$\Psi_{\xi'\xi'}+\Psi=(C_N^2/2\Psi^{1/2})-\Lambda , \tag{30}$$

where the rapidly varying part of R_1^2 has been neglected because its contribution to Ψ is small. Multiplying Eq. (30) by $\Psi_{\xi'}$ and integrating, one obtains

$$(\Psi_{\xi'})^2/2+G(\Psi)=K , \tag{31}$$

where

$$G(\Psi)=\Psi^2/2-C_N^2\Psi^{1/2}+\Lambda\Psi , \tag{32}$$

and K is an arbitrary constant. Equation (31) is of the same form as the energy conservation equation governing a particle with "energy" K, "position" Ψ, moving in a "potential" G with "time" ξ'. The "potential" $G(\Psi)$ is shown in Fig. 3 from which it is evident that, in order to obtain a solution Ψ which vanishes at turning points, it is necessary that the "energy" $K=0$. Furthermore, with $K=0$, Fig. 3 shows that Ψ has its maximum value Ψ_0 when G vanishes, i.e., $G(\Psi_0)=0$, whereby Eq. (32) yields the self-consistent relationship between the constants C_N and Ψ_0 as

$$C_N^2=\Psi_0^{3/2}/2+\Lambda\Psi_0^{1/2} . \tag{33}$$

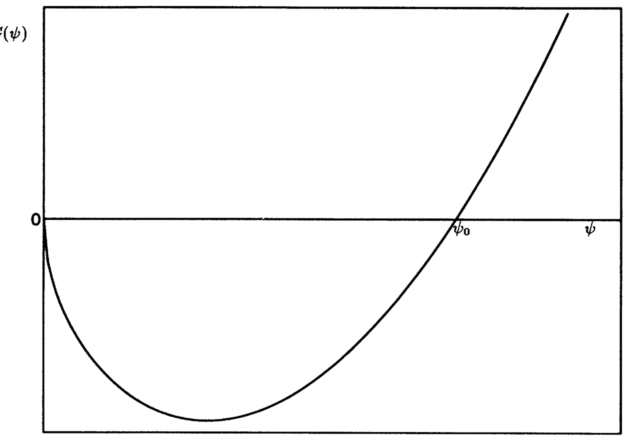

FIG. 3. Pseudopotential for solitary waves with $N \gg 1$.

From Fig. 2 and Table I it can be verified that, for large N,

$$\Lambda \ll \Psi_0/2 \ . \qquad (34)$$

Therefore, it is good approximation to neglect the term involving Λ in Eq. (33). Using Eq. (33) together with (34), one obtains from Eq. (31)

$$\xi' = \int_{\Psi}^{\Psi_0} \Psi^{-1/4}(\Psi_0^{3/2} - \Psi^{3/2})^{-1/2} d\Psi \qquad (35)$$

which, with the substitution $x = (\Psi/\Psi_0)^{3/4}$, can be integrated with the result

$$\Psi = \Psi_0 \cos^{4/3}(3\xi'/4) = \Phi_2 - \Lambda \approx \Phi_2 \ . \qquad (36)$$

Equation (36) gives the turning point locations (where Ψ vanishes) as

$$\pm \xi_0' = \pm 2\pi/3 \ , \qquad (37)$$

which agree closely with the locations obtained from Fig. 2 and Table I for large N. The constant Ψ_0 can be determined by substituting Eq. (36) into Eq. (28), which yields

$$\Psi_0^{1/2} \int_0^{2\pi/3} \cos^{2/3}(3\xi'/4) d\xi' = (2N-1)\pi/4 \ . \qquad (38)$$

With the evaluation of the integral [16], Eq. (38) gives

$$\Psi_0 = K_1 (N - \tfrac{1}{2})^2 \ , \qquad (39)$$

where

$$K_1 = [\Gamma^2(1/3)/2^{7/3}\Gamma(2/3)]^2 \approx 1.11 \ , \qquad (40)$$

and Γ is the gamma function. The function Ψ is now completely determined, and R_1 is determined from Eqs. (26), (33), and (36) with the result

$$R_1 = \tilde{R}_1 \sin\left[\int_0^{\xi'} \Psi^{1/2} d\xi' - N\pi/2\right] \ , \qquad (41)$$

$$\tilde{R}_1 = (K_1/2)^{1/2}(N - 1/2)\cos^{-1/3}(3\xi'/4) \ . \qquad (42)$$

Equations (36) and (41) are good approximations inside and not too near the turning points. The eigenvalue Λ can be determined by examining Φ_2 and R_1 near and to the right of the turning point ξ_0'. Near the turning point ξ_0' [15],

$$R_1 = -C_N \pi^{1/2} S^{-1/6} \mathrm{Ai}[S^{1/3}(\xi' - \xi_0')] \ , \qquad (43)$$

where S denotes the (unknown) magnitude of the slope of Ψ or Φ_2 at ξ_0', given by

$$S = -\Psi_{\xi'}(\xi_0') = -\Phi_{2\xi'}(\xi_0') \ , \qquad (44)$$

and Ai is the Airy function [17]. Thus, near the turning point, R_1 given by Eq. (26) connects smoothly onto R_1 given by Eq. (43). Also, the solution of Eq. (13) can be written in the form

$$\Phi_2(\xi') = \int_{\xi'}^{\infty} d\xi'' R_1^2(\xi'') \sin(\xi'' - \xi') \ , \qquad (45)$$

whose derivative is

$$\Phi_{2\xi'}(\xi') = -\int_{\xi'}^{\infty} d\xi'' R_1^2(\xi'') \cos(\xi'' - \xi') \ . \qquad (46)$$

Evaluating Eqs. (45) and (46) at the turning point ξ_0', and using $\Phi_2(\xi_0') = \Lambda$, $\Phi_{2\xi'}(\xi_0') = -S$, we obtain

$$\Lambda = \int_0^{\infty} dx\, R_1^2 \sin(x) \approx \int_0^{\infty} dx\, x R_1^2 \ , \qquad (47)$$

$$S = \int_0^{\infty} dx\, R_1^2 \cos(x) \approx \int_0^{\infty} dx\, R_1^2 \ , \qquad (48)$$

where $x = \xi' - \xi_0'$. The right-hand members of Eqs. (47) and (48) follow from the observation that, to the right of the turning point, R_1^2 decays in a distance $x \ll 1$, as is evident from Fig. 1. Because of the rapid decay of R_1^2 to the right of the turning point, the largest contribution to the integrals in Eqs. (47) and (48) come from the region near the turning point where Eq. (43) is assumed to be valid. Thus, Eqs. (47) and (48) become approximately

$$\Lambda = (\pi C_N^2 / S^{1/3}) \int_0^{\infty} \mathrm{Ai}^2(S^{1/3}x) x\, dx \ , \qquad (49)$$

$$S = (\pi C_N^2 / S^{1/3}) \int_0^{\infty} \mathrm{Ai}^2(S^{1/3}x) dx \ . \qquad (50)$$

The two Eqs. (49) and (50) in the two unknowns Λ and S are shown in the Appendix to yield

$$\Lambda \approx 0.197(N - \tfrac{1}{2})^{6/5} \ . \qquad (51)$$

Table I shows that Λ is very closely proportional to $(N - \frac{1}{2})^{6/5}$ as predicted by Eq. (51), but that the coefficient 0.197 in Eq. (51) is in error by about 40%. This error arises because Φ_2 is not truly linearly dependent on ξ' to the right of the turning point, as is evident in Fig. 2. Because of this, Eq. (43), which is based on the assumption of a linear dependence of Φ_2, is not an accurate approximation in the integrals of Eqs. (49) and (50). It should be noted, however, that, because $\Lambda \ll \Psi_0$, the error in Λ does not result in a significant error in $\Phi_2 = \Psi + \Lambda$, except near the turning points where Ψ given by Eq. (36) is already inaccurate because of the WKB approximation. Indeed, Fig. 4 shows that, for $N = 9$, Φ_2 obtained from Eqs. (36) and (51) is a very good approximation to the numerical solution except very near the turning point. Similarly, Fig. 5 shows that, for $N = 9$, Eq. (41) is also a good approximation for R_1 except very near the

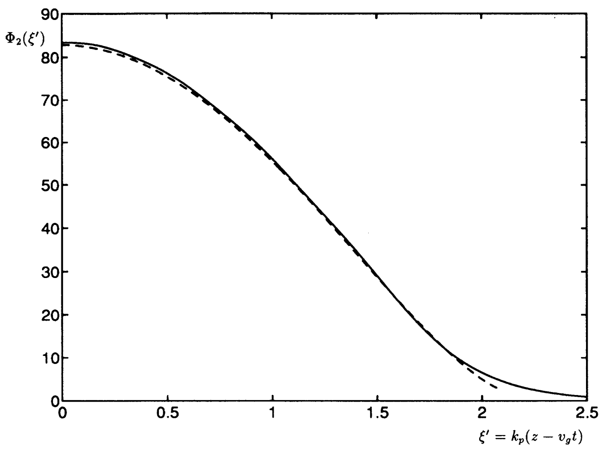

FIG. 4. For $N=9$, a comparison of the normalized scalar potential Φ_2 from numerical integration of Eqs. (12) and (13) (solid curve) with the approximate analytical result (dashed curve) obtained from $\Phi_2=\Psi+\Lambda$, where Ψ and Λ are given by Eqs. (36) and (51).

turning point. Moreover, it is evident from a comparison with the numerical solutions (not shown here) that, even for $N=2$, the approximate expressions for Φ_2 and R_1 derived here are remarkably accurate.

Using Eq. (41), the vector potential given by Eq. (22) becomes

$$A=\Omega_p\tilde{R}_1(\xi')[\exp(i\alpha_+)-\exp(i\alpha_-)]/2i+\text{c.c.}, \quad (52)$$

where

$$\alpha_\pm=\pm\int_0^{\xi'}(\Phi_2-\Lambda)^{1/2}d\xi'+KZ-\Omega T\mp N\pi/2 \ . \quad (53)$$

Thus, for large N, the vector potential is composed of two traveling waves with local frequencies and wave numbers given by

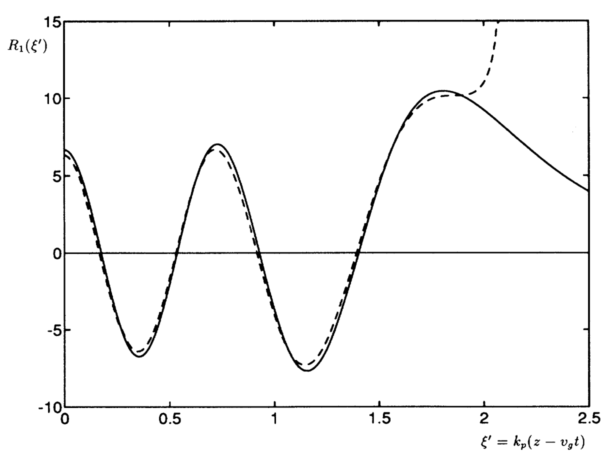

FIG. 5. For $N=9$, a comparison of the normalized vector-potential envelope R_1 from numerical integration of Eqs. (12) and (13) (solid curve) with the approximate analytical result given by Eq. (41) (dashed curve).

$$\Omega_\pm(\xi')=-\frac{\partial\alpha_\pm}{\partial T}=\Omega\pm\Omega_p\Omega_0'[\Phi_2(\xi')-\Lambda]^{1/2} \ , \quad (54)$$

$$K_\pm(\xi')=\frac{\partial\alpha_\pm}{\partial Z}=K\pm\Omega_p[\Phi_2(\xi')-\Lambda]^{1/2} \ , \quad (55)$$

where $\xi'=\Omega_p(Z-\Omega_0'T)$, and K and Ω are given by Eqs. (23) and (24). It is instructive to consider the phases $\alpha_\pm$, frequencies $\Omega_\pm$, and wave numbers $K_\pm$ in the group-velocity frame. Using the Lorentz transformation $Z=\gamma(\tilde{Z}+\Omega_0'\tilde{T})$, $T=\gamma(\tilde{T}+\Omega_0'\tilde{Z})$, $\gamma=[(1-(\Omega_0')^2]^{-1/2}=\Omega_0/\Omega_p$, one obtains, in terms of the group-velocity frame coordinate $\tilde{Z}$ and time $\tilde{T}$,

$$\alpha_\pm=\pm(\Omega_p^2/\Omega_0)\int_0^{\tilde{Z}}[\Phi_2(\xi')-\Lambda]^{1/2}d\tilde{Z} -\Omega_p(1-\Lambda\Omega_p^2/2)\tilde{T}\mp N\pi/2 \ , \quad (56)$$

where $\xi'=(\Omega_p^2/\Omega_0)\tilde{Z}$. Thus, the local frequencies and wave numbers in the group-velocity frame are

$$\tilde{\Omega}_\pm=-\frac{\partial\alpha_\pm}{\partial\tilde{T}}=\Omega_p(1-\Lambda\Omega_p^2/2)\approx\Omega_p(1-\Lambda\Omega_p^2)^{1/2} \ , \quad (57)$$

$$\tilde{K}_\pm(\xi')=\frac{\partial\alpha_\pm}{\partial\tilde{Z}}=\pm(\Omega_p^2/\Omega_0)[\Phi_2(\xi')-\Lambda]^{1/2} \ . \quad (58)$$

Equations (57) and (58) show that, in the group-velocity frame, the two traveling waves have identical frequencies but equal and opposite wave numbers, i.e., the vector potential consists of two oppositely traveling waves of equal amplitude. Moreover, the frequency is a constant whereas the wave numbers depend only on the spatial coordinate $\tilde{Z}$ (because of the $\tilde{Z}$ dependence of Φ_2), with the largest wave-number magnitude occurring at the center ($\tilde{Z}=0$) of the pulse. Because of the Doppler shift, the frequencies and wave numbers in the laboratory frame are dependent on both Z and T, as shown by Eqs. (54) and (55). Thus, the waves are considerably simpler when viewed in the group-velocity frame.

These solutions valid for large N can be related to the nonlinear dispersion relation which is

$$\Omega^2=K^2+\Omega_p^2(1-\Omega_p^2\Phi_2) \ , \quad (59)$$

where the relation $n/\gamma=1-\Omega_p^2\Phi_2$ has been used. Using the Lorentz transformation $\Omega=\gamma(\tilde{\Omega}+\Omega_0'\tilde{K})$, $K=\gamma(\tilde{K}+\Omega_0'\tilde{\Omega})$, $\gamma=\Omega_0/\Omega_p$, it can be shown that Eq. (59) also applies in the group-velocity frame,

$$\tilde{\Omega}^2+\tilde{K}^2+\Omega_p^2(1-\Omega_0^2\Phi_2) \ . \quad (60)$$

Inserting the frequency $\tilde{\Omega}$ given by Eq. (57) into the nonlinear dispersion relation (60), and solving for $\tilde{K}$, one obtains $\tilde{K}=\pm\Omega_p^2(\Phi_2-\Lambda)^{1/2}$ to lowest order in Ω_p, which agrees with Eq. (58) if we use the lowest-order approximation $\Omega_0\approx 1$. Therefore, it has been shown that the frequency and wave numbers given by Eqs. (57) and (58), as obtained from the approximate solution valid for large N, satisfy the nonlinear dispersion relation (60). Because of this, the nonlinear dispersion relation is useful to interpret the properties of the solution. In particular, Eqs.

(59) or (60) show that the normalized plasma frequency Ω_p is modified to $\tilde{\Omega}_p=\Omega_p(1-\Omega_p^2\Phi_2)^{1/2}$. This effect is produced by the combination of density modification due to the nonlinear generation of the longitudinal plasma wave and the nonlinear relativistic electron mass increase. Thus, a wave with a frequency $\tilde{\Omega}$ in the group-velocity frame propagates only if $\tilde{\Omega}>\tilde{\Omega}_p$. Because Eq. (57) shows that both waves comprising the solitary wave have a frequency $\tilde{\Omega}=\Omega_p(1-\Omega_p^2\Lambda)^{1/2}$, it follows that these waves propagate only if $\Phi_2>\Lambda$, which corresponds to the region between the two turning points. In the regions outside the turning points, where $\Phi_2<\Lambda$, the waves are purely evanescent, and decay exponentially. Thus, the nonlinear coupling of the electromagnetic pulse to the longitudinal plasma wave, whose scalar potential Φ_2 produces a modified plasma frequency $\tilde{\Omega}_p$ which is smaller in regions of larger Φ_2, creates a "cavity" between the two turning points in which the electromagnetic wave is trapped. Stated differently, the nonlinearly generated longitudinal plasma wave creates a region in which the local plasma frequency ($\propto n/\gamma$) is depressed. Since the electromagnetic wave can propagate only in regions were the local plasma frequency is below the wave frequency, it can be confined in this trough of depressed n/γ. Thus, the solitary wave solutions shown in Fig. 1 can be interpreted simply as eigenvalue solutions of the electromagnetic field in the bounded underdense trough between the two cutoff points at which the wave and plasma frequencies coincide.

Finally, it should be recognized that, although the solutions presented in this section are valid for large N, an upper limit on N does exist because a basic assumption of the perturbation theory on which the present analysis is based [14] is the condition $k_0 l \gg 1$, where l is the scale length on which the pulse envelope varies. From Fig. 1, it is evident that $l\sim(Nk_p)^{-1}$ for which the condition $k_0 l\gg 1$ becomes $N\ll\Omega_p^{-1}\approx\omega_0/\omega_p$.

IV. SUMMARY AND CONCLUSIONS

In summary, the properties of one-dimensional, linearly polarized, weakly nonlinear, electromagnetic solitary waves in a plasma are examined, based on a perturbation expansion in the small parameter $\epsilon\sim\Omega_p=\omega_p/k_0c\approx\omega_p/\omega_0\ll 1$. As in the strongly nonlinear case [12,13], the solitary waves are obtained from the eigenvalues and eigenfunctions of a system of two coupled equations. Contrary to the strongly nonlinearly case, however, the governing equations are much simpler, and their solutions result in the following general properties of these weakly nonlinear solitary waves. The $N=1$ case, where N denotes the number of half-cycles of the vector-potential envelope, is the only solitary wave whose width is large compared with the plasma wavelength, but is a true wakeless solitary wave only for vanishing amplitude. The solitary waves with $N\geq 2$ all have widths comparable to the plasma wavelength, and are increasingly oscillatory with increasing N. The normalized vector-potential envelope and scalar potential are obtained by multiplying the universal curves in Figs. 1 and 2 by Ω_p and Ω_p^2, respectively. Thus, the vector- and scalar potential amplitudes of each solitary wave have discrete values which are proportional to Ω_p and Ω_p^2, respectively. The interaction of the laser pulse with the plasma produces nonlinear frequency and wave-number shifts given in Eqs. (23) and (24). Through second order in Ω_p^2, the group and phase velocities are shown to satisfy $v_g v_p=c^2$.

Equations (36) and (41) give simple analytic expressions for the scalar potential Φ_2 and the vector-potential envelope R_1 for $N\gg 1$. Moreover, Eq. (52) shows that, between the turning points, the solitary wave for $N\gg 1$ can be considered to consist of the sum of two traveling waves with different local wave numbers and frequencies which are dependent on both Z and T. When viewed in the group-velocity frame, however, these two traveling waves have identical constant frequencies but equal and opposite local wave numbers which depend only on the spatial coordinate. Furthermore, these waves are trapped between the two turning points at which the nonlinearly modified local plasma frequency is equal to the wave frequency.

ACKNOWLEDGMENTS

This work was partly supported by U.S. DOE under Grant No. DE-FG03-92-ER40727.

APPENDIX: DERIVATION OF EQ. (51)

Letting $y=S^{1/3}x$, Eqs. (49) and (50) become

$$\Lambda=(\pi C_N^2/S)\int_0^\infty \mathrm{Ai}^2(y)y\,dy\ , \tag{A1}$$

$$S=(\pi C_N^2/S^{2/3})\int_0^\infty \mathrm{Ai}^2(y)dy\ . \tag{A2}$$

To evaluate the integrals in Eqs. (A1) and (A2), we use the differential equation for $w(y)=\mathrm{Ai}^2(y)$, which is [17]

$$w_{yy}-4yw_y-2w=0\ . \tag{A3}$$

Integrating Eq. (A3) between the limits 0 and ∞, and using integration by parts, one obtains

$$\int_0^\infty w\,dy=w_{yy}(0)/2=[\mathrm{Ai}'(0)]^2\ . \tag{A4}$$

Similarly, multiplying Eq. (A3) by y and integrating, one obtains

$$\int_0^\infty wy\,dy=-w_y(0)/6=-\mathrm{Ai}(0)\mathrm{Ai}'(0)/3\ . \tag{A5}$$

Using Eqs. (A4) and (A5) together with [17] $\mathrm{Ai}(0)=3^{-2/3}/\Gamma(2/3)$ and $\mathrm{Ai}'(0)=-3^{-1/3}/\Gamma(1/3)$, Eqs. (A1) and (A2) become

$$\Lambda=\pi C_N^2/9S\Gamma(1/3)\Gamma(2/3)\ , \tag{A6}$$

$$S=\pi C_N^2/3^{2/3}S^{2/3}\Gamma^2(1/3)\ . \tag{A7}$$

Eliminating S from Eqs. (A6) and (A7) and using Eqs. (33) and (39), we obtain

$$\Lambda=\left[\frac{\pi^2\Gamma^{13}(1/3)(N-\frac{1}{2})}{3^8 2^{16}\Gamma^{11}(2/3)}\right]^{1/5}, \tag{A8}$$

which, with numerical values inserted, yields Eq. (51).

[1] T. Tajima and J. M. Dawson, Phys. Rev. Lett. **43**, 267 (1979).
[2] R. Ruth, A. Chao, P. Morton, and P. Wilson, Part. Accel. **17**, 171 (1985).
[3] R. Keinigs and M. E. Jones, Phys. Fluids **30**, 252 (1987).
[4] P. Chen, J. M. Dawson, R. W. Huff, and T. Katsouleas, Phys. Rev. Lett. **54**, 693 (1985).
[5] C. E. Max, J. Arons, and A. B. Langdon, Phys. Rev. Lett. **33**, 209 (1974).
[6] S. C. Wilks, J. M. Dawson, W. B. Mori, T. Katsouleas, and M. E. Jones, Phys. Rev. Lett. **62**, 2600 (1989).
[7] P. Sprangle, E. Esarey, and A. Ting, Phys. Rev. A **41**, 4463 (1990).
[8] J. I. Gersten and N. Tzoar, Phys. Rev. Lett. **35**, 934 (1975).
[9] N. L. Tsintsadze and D. D. Tskhakaya, Zh. Eksp. Teor. Fiz. **72**, 480 (1977) [Sov. Phys. JETP **45**, 252 (1977)].
[10] M. Y. Yu, P. K. Shukla, and K. H. Spatschek, Phys. Rev. A **18**, 1591 (1978).
[11] N. N. Rao, R. Varma, P. K. Shukla, and M. Y. Yu, Phys. Fluids **26**, 2488 (1983).
[12] V. A. Kozlov, A. G. Litvak, and E. V. Surorov, Zh. Eksp. Teor. Fiz. **76**, 148 (1979) [Sov. Phys. JETP **49**, 75 (1979)].
[13] P. K. Kaw, A. Sen, and T. Katsouleas, Phys. Rev. Lett. **68**, 3172 (1992).
[14] H. H. Kuehl, C. Y. Zhang, and T. Katsouleas, Phys. Rev. E **47**, 1249 (1993).
[15] P. M. Morse and H. Feshbach, *Methods of Theoretical Physics* (McGraw-Hill, New York, 1953), p. 1092.
[16] I. S. Gradshteyn and I. M. Ryzhik, *Tables of Integrals, Series, and Products* (Academic, New York, 1980), p. 948.
[17] H. A. Antosiewicz, in *Handbook of Mathematical Functions,* edited by M. Abramowitz and I. A. Stegun, Natl. Bur. Stand. App. Math. Ser. No. 55, (U.S. GPO, Washington, DC, 1964), Sect. 10.4.